

The intelligent catalyst having the self-regenerative function of Pd, Rh and Pt for automotive emissions control

Hirohisa Tanaka^{a,*}, Mari Uenishi^a, Masashi Taniguchi^a, Isao Tan^a, Keiichi Narita^b, Mareo Kimura^b, Kimiyoshi Kaneko^c, Yasuo Nishihata^d, Jun'ichiro Mizuki^d

^aMaterials Research and Development Division, Daihatsu Motor Co. Ltd., Ikeda, Osaka 563-8651, Japan

^bResearch and Development Division, Cataler Corporation, Kakegawa, Shizuoka 437-1492, Japan

^cFine Chemical Research Laboratories, Hokko Chemical Industry Co. Ltd., Atsugi, Kanagawa 243-0023, Japan

^dKansai Photon Science Institute, Japan Atomic Energy Agency, Sayo, Hyogo 679-5148, Japan

Available online 23 June 2006

Abstract

The self-regenerative function of precious metals in the intelligent catalyst is an epoch-making technology in the history of automotive catalysts after the 1970's. The mechanism of the self-regenerative function is studied by X-ray absorption fine-structure (XAFS) analyses. The function was realized through a cyclic movement of Pd between the outside (as Pd nanoparticles) and the inside (as Pd cations in the lattice) of the perovskite crystal in synchronization with the inherent fluctuations between reductive and oxidative (redox) atmospheres that occur in real automotive exhaust gases. As the result, the growth of Pd particles can be suppressed during the entire lifetime of the vehicle. Moreover, the speed of this function was measured at the time resolution of a 10 ms by *in situ* energy dispersive XAFS, and it is proved that the self-regenerative function occurs at an extremely high speed. Furthermore, the new perovskite catalysts which have the self-regenerative function of Rh and Pt, as well as Pd, are discussed here. This self-regenerative function provides a new and useful tool for designing the future catalyst technology.

© 2006 Elsevier B.V. All rights reserved.

Keywords: Perovskite; Catalyst; Palladium; Rhodium; Platinum; Self-regeneration; Automotive emission; XAFS; *In situ* experiment

1. Introduction

An ageless catalyst is a kind of philosopher's stone for automotive engineers. In this paper, the newest research on a self-regenerative intelligent catalyst is described. The catalyst has the ability to regain its catalytic activity, should this deteriorate, in the use environment without any auxiliary treatment [1–5]. From the viewpoint of “intelligent materials” [6], the intelligence of the catalyst may be defined as its ability to maintain a high performance by adapting its structure, responding sensitively to environmental changes.

The important role of the automotive three-way catalyst is widely recognized for the simultaneous conversion of emissions of three pollutants in engine exhaust gases, carbon monoxide (CO), nitrogen oxides (NO_x), and unburned hydrocarbons (HC) into harmless non-pollutants. The conven-

tional three-way catalyst consists of fine particles of precious metals dispersed on ceramic support materials such as alumina, ceria, and zirconia. However, the catalytic activity of such catalysts deteriorates, owing to the agglomeration and growth of precious metal particles during use. It is essential to suppress the growth of precious metal particles to achieve a high efficiency and to conserve precious metals.

Automotive emissions regulations are getting tighter and tighter all over the world. The Japanese government has introduced cleaner emission standards, designated ultra-low-emission vehicle (J-ULEV) and a new super-ultra-low-emission vehicle (J-SULEV), which involve, respectively, 50% and 75% reductions in emissions of both HC and NO_x in comparison with the emission regulation 2005. More and more precious metals must be used to meet these severe standards when conventional catalyst technologies are applied. In particular, the demand for Pd for use in automotive catalysts has increased explosively from 15 to over 150 t per year [7]. This drastic increase is a result of the strengthening of cold-emission regulations world wide, which has made development

* Corresponding author. Fax: +81 72 754 3444.

E-mail address: hirohisa_tanaka@mail.daihatsu.co.jp (H. Tanaka).

of technologies to reduce the use of precious metals so urgent. The objective of the development of the intelligent catalyst is to reduce of palladium use in automotive industries, and to adjust these demands proportion into the natural source ratio of Pd, Pt, and Rh.

The intelligent Pd-perovskite catalyst has a greatly improved durability as a result of the self-regenerative function of Pd nano-particles. It has been confirmed that the catalytic activity can be maintained even when the amount of precious metals is reduced by 70–90% [8,9]. A vehicle equipped with the intelligent catalyst was supplied to the market and succeeded in achieving J-ULEV standard in 2002. Moreover, the intelligent catalyst has also succeeded in achieving a new J-SULEV standard, adopted promptly from January 2004. The production of clean vehicles equipped with the intelligent catalyst exceeded 1.5 million units in September 2005. By this technology, it not only became possible to achieve a drastic reduction in the cost of catalysts, but also the technology solved the problem of the supply and demand of precious metals for automotive applications, which had caused a negative effect on other industries. The intelligent catalyst now attracts worldwide attention and provides a new concept for designing the future catalyst technology. In this paper, Pd-intelligent catalyst technology is described in detail, including the brand new result of *in situ* synchrotron experimental. In addition, it is further discussed about progressive development of the technology into Rh and Pt.

2. Elucidation of the self-regenerative function of palladium-perovskite

A palladium-containing perovskite ($\text{LaFe}_{0.95}\text{Pd}_{0.05}\text{O}_3$; Pd-perovskite) powder catalyst was prepared by the alkoxide method [1,3]. Lanthanum and iron ethoxyethylates $\{\text{M}^{3+}(\text{OC}_2\text{H}_4\text{OC}_2\text{H}_5)_3$ ($\text{M} = \text{La}^{3+}$ and Fe^{3+}) $\}$ were dissolved in toluene. Palladium acetylacetonate $\{\text{Pd}^{2+}(\text{CH}_3\text{COCH}(\text{COCH}_3)_2)\}$ was also dissolved in toluene. The amount of Pd was adjusted to 5 at.% of that of the B-site element of the perovskite structure. Precipitate containing Pd was obtained by hydrolysis with deionized water. The precursor was dried and then calcined at 800 °C for 2 h in an air to obtain

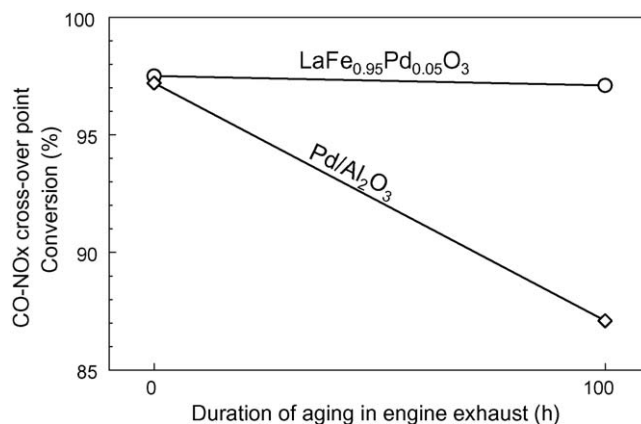


Fig. 1. CO-NOx cross-over point conversion.

$\text{LaFe}_{0.95}\text{Pd}_{0.05}\text{O}_3$ perovskite powder catalyst containing homogeneously distributed precious metal. To prepare the conventional catalysts, powdered $\gamma\text{-Al}_2\text{O}_3$ ($\text{SSA} = 120 \text{ m}^2 \text{ g}^{-1}$) was impregnated with dilute aqueous palladium nitric acid $\{\text{Pd}(\text{NO}_3)_2\}$, dried, and calcined at 500 °C for 1 h in an air.

$\text{LaFe}_{0.95}\text{Pd}_{0.05}\text{O}_3$ and $\text{Pd}/\gamma\text{-Al}_2\text{O}_3$ powders were coated on the inner wall of a monolithic honeycomb substrate (80 mm in diameter and 95 mm in length with the grid of 64 cell cm^{-2}), containing the same amounts of Pd (3.26 mg cm^{-3}) [1]. The two monolithic catalysts were attached to each side bank in the exhaust system of an automotive 4000 cm^3 V-8 engine for simultaneous ageing treatment. The monolithic catalysts were then exposed to high-temperature exhaust gas at 900 °C for 100 h, by the alternation of a large redox fluctuating atmosphere ($\Delta\lambda = \pm 4\%$ at 0.6 Hz) around the stoichiometric point for 870 s and an oxidation atmosphere for 30 s. This ageing procedure is widely accepted as simulating a driving strategy for achieving a high fuel economy by introducing fuel cutoff during deceleration.

Fig. 1 compares the CO-NOx crossover point conversion of these aged catalysts. The $\text{LaFe}_{0.95}\text{Pd}_{0.05}\text{O}_3$ catalyst maintained its high activity during aging, the same as $\text{LaFe}_{0.57}\text{Co}_{0.38}\text{Pd}_{0.05}\text{O}_3$, whereas the activity of the Pd/alumina catalyst deteriorated by about 10% [1]. Transmission electron microscopy (TEM) images of the aged catalysts are shown in Fig. 2 [10–12]. The Pd particles

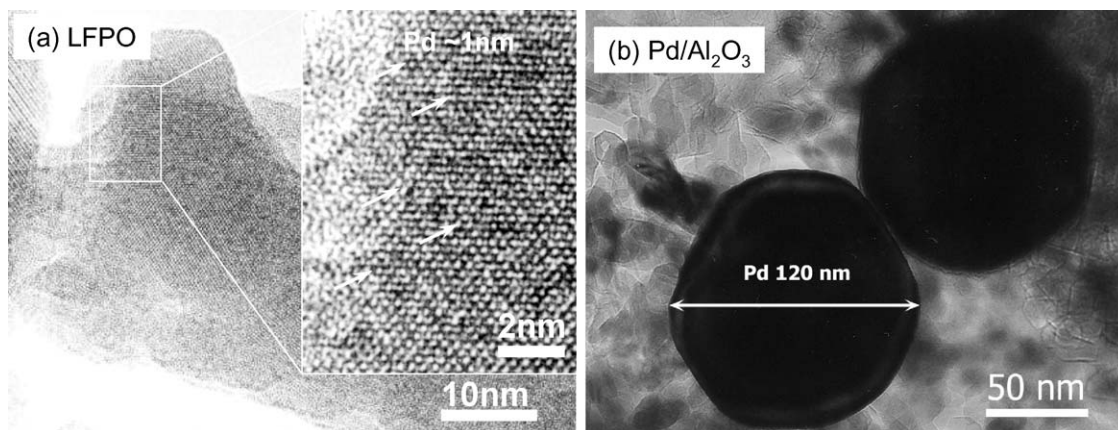


Fig. 2. TEM observation of Pd on catalysts after engine aging at 900 °C.

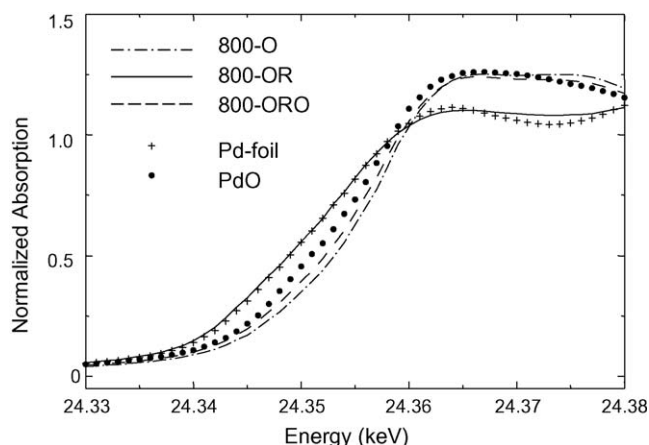


Fig. 3. XANES Spectra of Pd K-edge for $\text{LaFe}_{0.95}\text{Pd}_{0.05}\text{O}_3$.

on alumina reached sizes of up to 120 nm, whereas only small metallic particles of about 1 nm in diameter were found on the perovskite surface. The remarkable suppression of the growth of metallic particles directly affects the ability of the Pd-perovskite catalyst to maintain a high catalytic activity.

In order to explain this unique phenomenon, X-ray absorption fine structure (XAFS) analysis was carried out at the bending-magnet beam lines BL01B1 and BL14B1 of the 8-GeV synchrotron radiation source in SPring-8, Japan. The powder for the measurement was exposed to the following treatments. First, the catalyst was oxidized in air at 800 °C for 1 h (800-O). Secondly, the sample was reduced in 2.5% H_2 and 7.5% CO balanced with N_2 for 1 h at 100, 200, 300, 400, 600, or 800 °C (100-OR, 200-OR, 300-OR, 400-OR, 600-OR and 800-OR). Finally, the sample was re-oxidized in air for 1 h at the same temperatures as in the reduction treatment (100-ORO, 200-ORO, 300-ORO, 400-ORO, 600-ORO and 800-ORO) [12–17]. This successive treatment creates a separate model for each of the key stages of the evolution of the engine exhaust atmosphere at various temperatures. The XAFS spectra were measured near the Pd–K edge in transmission mode because of the high transmissivity of the X-ray. The photon energy was calibrated with a Pd foil by assigning the half of edge jump as 24.350 keV. Fig. 3 shows X-ray absorption near-edge structure (XANES) spectra of the Pd–K edge for $\text{LaFe}_{0.95}\text{Pd}_{0.05}\text{O}_3$ perovskite, after oxidation, reduction, and re-oxidation treatments at 800 °C, together with the XANES spectra of Pd-foil and PdO as reference materials [18].

The local structure parameters of the first nearest neighbor around the Pd in $\text{LaFe}_{0.95}\text{Pd}_{0.05}\text{O}_3$ after redox treatments at 800 °C are shown in Table 1 [18]. The temperature dependency

of the radial structure function around Pd is shown in Fig. 4 [12–16]. At first, Pd in the sample oxidized at 800 °C (800-O) occupied the B-site, in the six-fold coordination with oxygen, of the unit formula of ABO_3 in the perovskite structure. When the sample was reduced and Pd was segregated from the perovskite crystal to form small metallic particles, the first nearest peak height corresponding to the Pd–O bond decreased, and the second peak corresponding to the Pd–Pd bond increased as the reduction temperature increased from 200 °C. At 800 °C, the peak showed a mixture of Pd–Pd and Pd–Fe bonds (800-OR). Note that the summation of the weight of both the Pd–Pd and Pd–Fe bonds is only 0.64, implying that the deposited metal particle is very small. In a re-oxidation atmosphere, the height of the Pd–Pd bond decreased from 200 °C (Fig. 5) [18]. After re-oxidation at 800 °C (800-ORO), the Pd–Pd bond disappeared, and the local structure around Pd was identical to that of the oxidized catalyst (800-O).

For comparison with XAFS, the behavior of surface Pd in the reduction treatment was also analyzed by X-ray photoelectron spectroscopy (XPS). This showed that the ratio of metallic Pd on the surface is higher than that in the bulk structure within the temperature range 100–300 °C (Fig. 5) [12–14,17]. This suggests that reductive segregation of Pd begins near the surface, and then Pd from the bulk of the perovskite framework segregates later. The results of XAFS and XPS analyses indicate that Pd of the $\text{LaFe}_{0.95}\text{Pd}_{0.05}\text{O}_3$ perovskite moves in a completely reversible manner during sequential redox fluctuations. In addition, it is revealed that this regenerative function of Pd occurs from very low temperatures [13,17]. The mechanism of the self-regenerative function is illustrated in Fig. 6 [9].

3. Direct observation of rapid movement of palladium

It became clear that a Pd-perovskite catalyst can maintain high activity according to the grain growth control effect of Pd by the self-regeneration function. There are two left-behind big questions here. The first question: Can this movement of Pd respond a quick change like reduction-oxidation fluctuation of an actual automotive engine exhaust gas? The second question: Is this self-regeneration function the special phenomenon, which may happen only to Pd? Or is it possible to develop as universal catalyst technology, which may happen also to Rh and Pt? In order to answer the first question, the *in situ* measurement using energy dispersive XAFS (DXAFS) was carried out at beamline ID-24 in ESRF, France [19]. The spectra were consecutively measured in 10 ms time resolution. The silicon

Table 1
Local structure parameters around Pd of $\text{LaFe}_{0.95}\text{Pd}_{0.05}\text{O}_3$ treated at 800 °C estimated by EXAFS [18]

K-edge	Ageing treatment	Shell (bond)	Weight (W_{shell})	Coordination number	Interatomic distance (nm)	Debye–Waller factor ($\times 10^{-4} \text{ nm}^2$)	Discrepancy factor (%)
Pd	800-O	Pd–O	1	6*	0.2038 (5)	0.58 (3)	3.9
	800-OR	Pd–Fe/Pd–Pd	0.44	6*/6*	0.2683 (3)	0.64 (4)	8.6
		Pd–Pd	0.20	12*	0.2743 (1)	0.64†	
	800-ORO	Pd–O	1	6*	0.2038 (5)	0.65 (3)	8.9

The parameter marked with * was fixed. The parameter marked with † was treated as the same value for the other shell.

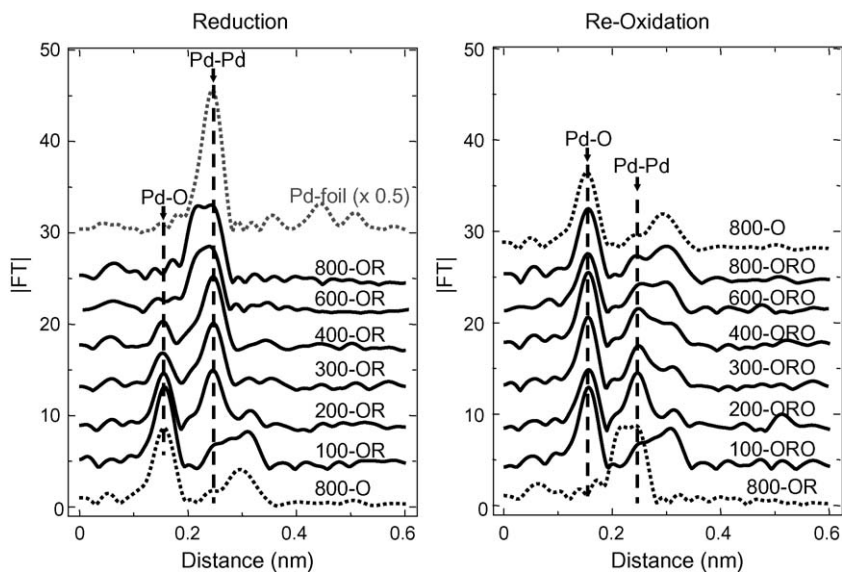


Fig. 4. Radial structure function around Pd of $\text{LaFe}_{0.95}\text{Pd}_{0.05}\text{O}_3$.

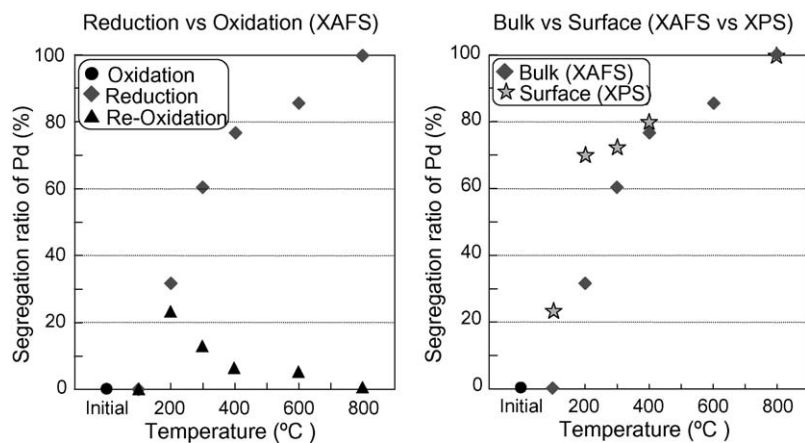


Fig. 5. Ratio of metallic Pd for $\text{LaFe}_{0.95}\text{Pd}_{0.05}\text{O}_3$ [15–17].

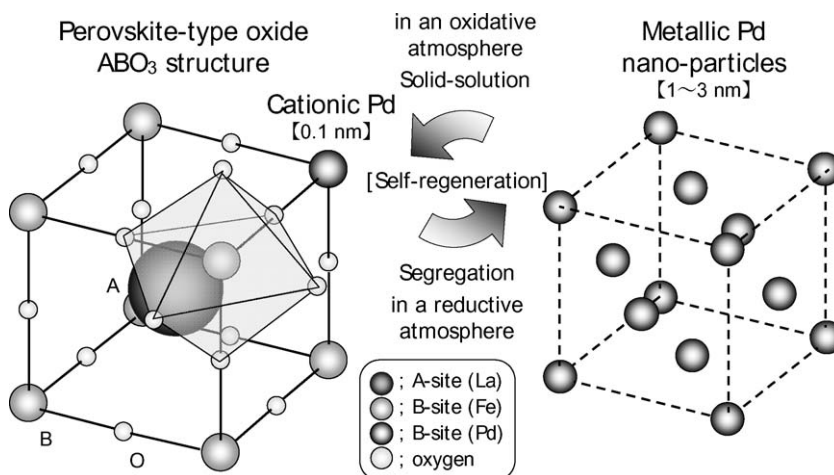


Fig. 6. Self-regenerative function of the intelligent catalyst [9].

Table 2
Gas condition for *in situ* DXAFS experiment

Gas condition	Real auto-exhaust	<i>In situ</i> experiment
Total gas flow ($\text{cm}^3 \text{min}^{-1}$)	2×10^6	100
Reducing gas concentration (%)	4	50
Amount of Pd (g piece^{-1})	0.3	0.2×10^{-3}
Reducing gas/Pd ($\text{cm}^3 \text{g}^{-1} \text{min}^{-1}$)	$2 \times 10^6 \times 0.04/0.3 = 2.6 \times 10^5$	$100 \times 0.50/(0.2 \times 10^{-3}) = 2.5 \times 10^5$

polychromator crystal was set to the Bragg configuration with (3 1 1) to obtain dispersed X-ray beam near Pd K-edge (24.350 keV). A CCD camera was used as a detector to observe a fluorescent screen [19,20].

For DXAFS, $\text{LaFe}_{0.9}\text{Pd}_{0.1}\text{O}_3$ and $\text{Pd}/\gamma\text{-Al}_2\text{O}_3$ containing the same amount (4.3 mass%) of Pd were prepared by the alkoxide method. A pellet of each sample was placed in quartz *in situ* cells ($\phi = 5.0 \text{ mm}$); 50% O_2 (balanced with He) was used as the oxidizing gas and 50% H_2 (balanced with He) was used as the reducing gas. The total gas flow rate was set at $100 \text{ cm}^3 \text{min}^{-1}$. This condition was considered to be equivalent to an actual engine-exhaust gas (Table 2) [21]. A thermal conductivity detector (TCD), which detected the gases' change, was set in front of the pellet to send the trigger signal starting the measurement. Just after switching the gas flow from oxidizing through He to reducing, and from reducing through He to oxidizing, the spectra were measured with a 10 ms-resolution during 5 s at a programmed temperature of $400 \text{ }^\circ\text{C}$. After measurement under oxidizing conditions, the temperature was raised to $700 \text{ }^\circ\text{C}$ in keeping an oxidizing gas flow for 30 s, to completely restore the precious metal to the perovskite structure. The measurement was carried out continuously over 10 repetitions of the reducing–oxidizing cycle.

Fig. 7 shows the temporal dependence of coordination number (CN) of Pd–O and Pd–Pd bonds. The CN of Pd–O for LaFePdO_3 originated from the B-site of the perovskite structure is 6, while that of Pd–O bond for $\text{Pd}/\text{Al}_2\text{O}_3$ originated from PdO is 4. The CN of Pd–Pd bond originated from the metallic Pd

should be 12 theoretically. In the reduction process, the CN of the Pd–O bond for LaFePdO_3 perovskite rapidly decreases, and over 80% of Pd in the perovskite crystal was reduced at $400 \text{ }^\circ\text{C}$. Of particular interest, the generation of Pd–Pd bonds in LaFePdO_3 was instantaneous, and the CN of Pd–Pd bond was maintained with the small value about 6 after 1 s. The diameter of metallic Pd particles segregated from LaFePdO_3 was calculated to be about 0.8 nm. On the other hand, the CN of the Pd–Pd bond of $\text{Pd}/\text{Al}_2\text{O}_3$ increased continuously, and it was estimated to be 8, corresponding to about 1.3 nm of diameter. Specific surface area (SSA) of $\text{Pd}/\text{Al}_2\text{O}_3$ was ten times as large as that of LaFePdO_3 . However, the Pd particles size of LaFePdO_3 is smaller. It was thought that there was a certain interaction between Pd particles and LaFePdO_3 matrix. The CN changes both of Pd–O and Pd–Pd bonds for LaFePdO_3 were faster than the changes for $\text{Pd}/\text{Al}_2\text{O}_3$. That is, the redox changes in Pd that accompany its segregation from the perovskite crystal are faster than the simple reduction from PdO to Pd on alumina. Here it is proved that the dynamic movements of Pd with the perovskite crystal can respond to the control frequency (1–4 Hz) of an actual gasoline engine.

4. Self-regenerative function of rhodium and platinum

To study the self-regenerative properties, perovskite catalysts containing Rh or Pt were prepared by the alkoxide method. The oxidation (O), reduction (OR) and re-oxidation (ORO) treatments of the catalyst were carried out at $800 \text{ }^\circ\text{C}$. XAFS measurements were also carried at BL-01B1 and BL-14B1 in SPring-8, to determine the distribution of Rh and Pt in the perovskite crystal structure [22].

The XANES spectrum near Rh K-edge for $\text{LaFe}_{0.95}\text{Rh}_{0.05}\text{O}_3$ after each treatment is shown in Fig. 8a, and the calculated radial structure function around Rh is shown in Fig. 8b. All the Rh of $\text{LaFe}_{0.95}\text{Rh}_{0.05}\text{O}_3$ was present as a solid-solution in perovskite after oxidation, but it segregated with about 35% of Rh even after reduction at $800 \text{ }^\circ\text{C}$. By replacing the perovskite from $\text{La}^{3+}\text{Fe}^{3+}\text{O}_3$ to $\text{Ca}^{2+}\text{Ti}^{4+}\text{O}_3$, the segregation of metallic Rh particles after reduction is significantly improved (Fig. 9b). The XANES spectrum near the Rh K-edge for reduced

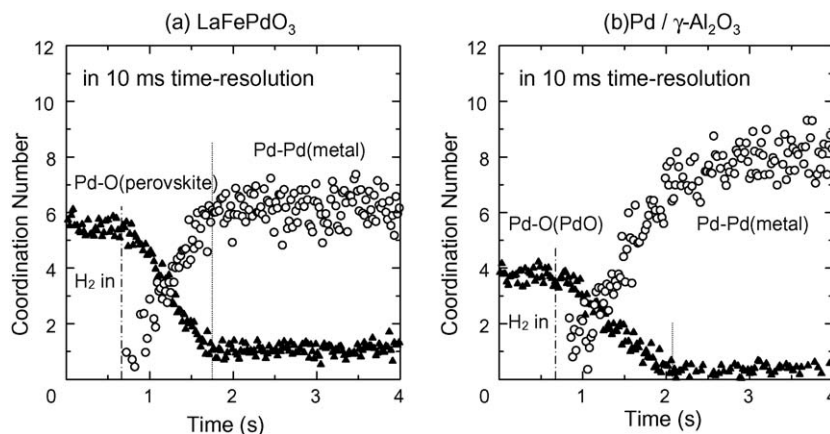
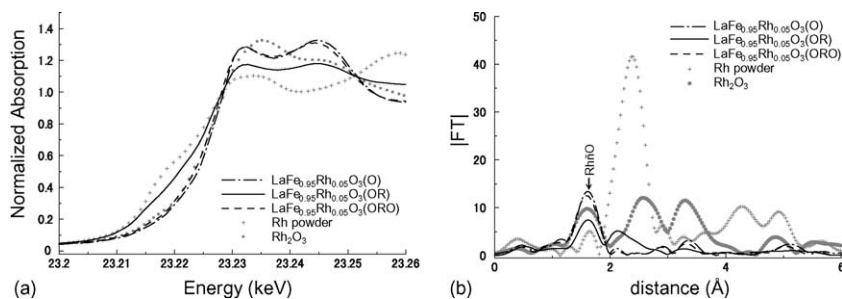


Fig. 7. *In situ* DXAFS at $400 \text{ }^\circ\text{C}$ in reduction process.

Fig. 8. XANES Spectra of Rh K-edge for LaFeRhO₃ [22].

CaTi_{0.95}Rh_{0.05}O₃ shifted towards the energy for metallic Rh powder, implying that a greater proportion of Rh segregates and is in the metallic state (Fig. 9a).

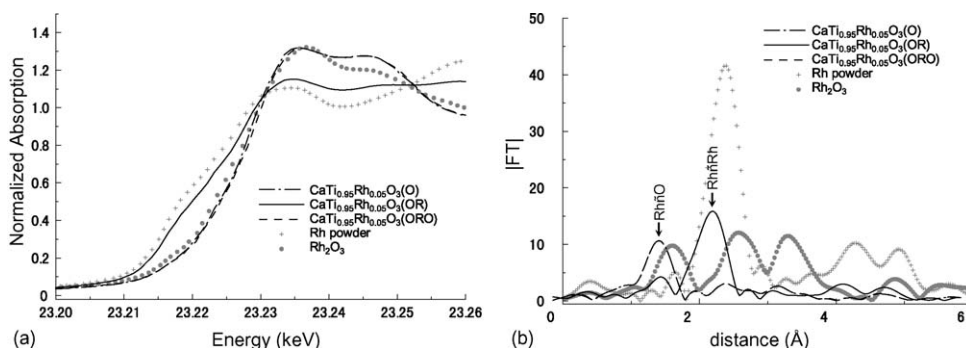
The XANES spectrum near Pt L_{III}-edge for CaTi_{0.95}Pt_{0.05}O₃ after each treatment is shown in Fig. 10a, and the calculated radial structure function around Rh is shown in Fig. 10b. All the Pt of CaTi_{0.95}Pt_{0.05}O₃ was present as a solid-solution in perovskite in oxidation, segregated to metallic Pt particles in reduction, and the Pt particles were restored in the perovskite framework completely in re-oxidation at 800 °C. Thus, CaTi_{0.95}Rh_{0.05}O₃ and CaTi_{0.95}Pt_{0.05}O₃ show the excellent self-regeneration function. The A²⁺B⁴⁺O₃ perovskites, of which CaTiO₃ is a natural mineral representative, are not considered to have catalytic activity. It is mentioned especially that the various oxides, which were not used as a catalyst until now, can be used effectively. However, neither Rh nor Pt forms a solid solution in SrZrO₃, and not all A²⁺B⁴⁺O₃ perovskite-type oxides are effective [22].

Finally, the effect on the suppression of growth of Pt particles in an actual engine exhaust gas was investigated. CaTi_{0.98}Pt_{0.02}O₃ and Pd/γ-Al₂O₃ catalysts were exposed to actual engine exhaust gas at 900 °C for 100 h and then the Pt particles were examined by transmission electron microscopy (TEM) (Fig. 11) [22]. The Pt particles on alumina grew to over 100 nm, whereas only fine metallic particles about 1–3 nm in diameter were found on the perovskite surface. It is proved that a precious metal-containing perovskite catalyst can function as an intelligent catalyst that regenerates itself and maintains a high activity by the cycle forming a solid-solution and segregation even in a harsh redox environment at high

temperatures where precious metals normally suffer grain growth, causing deterioration in their catalytic activity.

It is confirmed that the precious metals Pd, Rh, and Pt in a Intelligent catalyst move back and forth between the B-site in the perovskite structure and the metallic nanoparticles when exposed to inherent redox fluctuations of the actual engine exhaust, and thus the catalytic activity is maintained during the lifetime of a vehicle (Fig. 12). The perovskite-type oxides are very useful because of their structural stability and the abundance of possible combinations. In designing an intelligent catalyst, the following technology is important. The oxide, which makes perovskite representative, should maintain a stable structure to heal the precious metal at high temperatures in a redox environment. Under reductive conditions, the precious metal emerges from the framework of the perovskite to form metallic clusters or nanoparticles. Under oxidative conditions, the precious metal comes back to the perovskite framework to refresh itself. The precious metal repeats the cycle of solid solution and segregation responding to the inherent cycling between an oxidative and a reductive environment.

In addition, a self-regenerative Pd-perovskite catalyst has been reported by the research group of S.V. Ley and M.D. Smith to show a high activity and a long life in organic synthesis reactions, such as the Suzuki coupling [23,24]. The applications of this technology could be extended not only to pharmaceutical synthesis, but also to a diesel after-treatment; such technology will be in increasing demand as it solves the socioeconomic problem relating to the supply and demand for precious metals.

Fig. 9. XANES Spectra of Rh K-edge for CaTiRhO₃ [22].

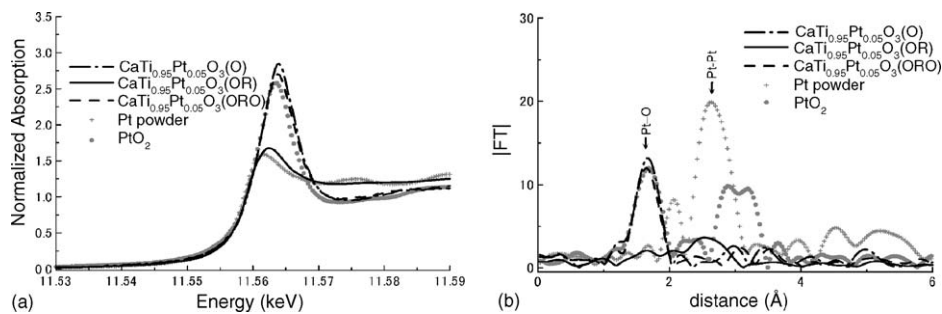


Fig. 10. XAFS Spectra of Pt L_{III}-edge for CaTiPtO₃.

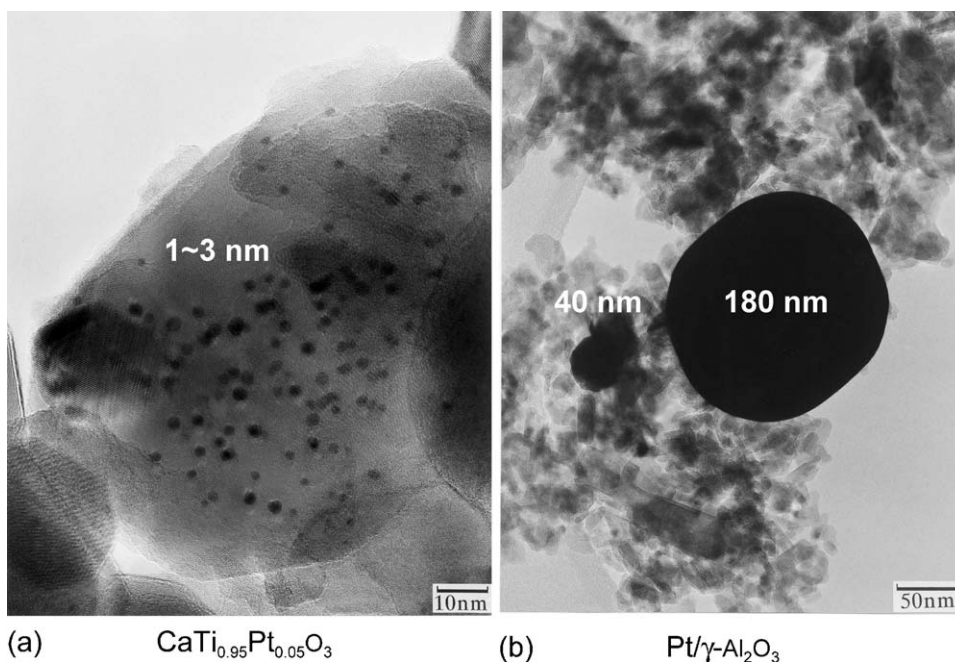


Fig. 11. TEM observation of Pt on catalysts after engine aging at 900 °C [22].

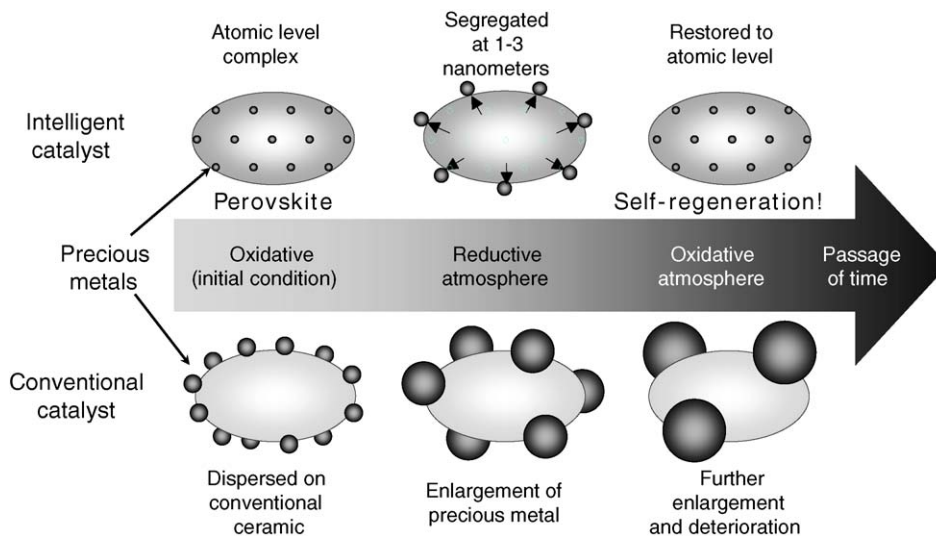


Fig. 12. Suppression of the growth of precious metal particles [12].

5. Conclusion

The modern gasoline engine has adopted a feedback control system that uses an oxygen sensor for three-way catalysts to function, and the oxygen concentration of the exhaust gas component is always fluctuating. In the intelligent catalyst, all the precious metals used in automotive catalysts, Pd, Rh and Pt, are always rejuvenated itself into an active state in a rapid fluctuation typically encountered in the exhaust gas from the gasoline engine, and thereby degradation of the catalyst is prevented. The intelligent catalyst provides a new material design technology, and it is expected that this technology will contribute considerably to the solution of the supply-and-demand problems of precious metals in the automotive industries. The intelligent catalyst is also expected to be an important technology, not only for automobiles, but also for various internal combustion engines. By further development of this technology, a vehicle that emits an exhaust gas that is cleaner than ambient air could be achieved. Intelligent catalyst technology is expected to be the key that opens the window for clean air to blow in.

Acknowledgements

The authors would like to thank Professor Emeritus Dr. M. Misono of the University of Tokyo and Professor Dr. T. Kobayashi of National Institute of Advanced Industrial Science and Technology (AIST) for their guidance. The authors wishes sincerely to express their deep gratitude to Dr. S. Pascarelli, Dr. M. Newton and Dr. G. Guilera of European Synchrotron Radiation Facility (ESRF), Dr. T. Uruga, Mr. K. Kato and Ms. Y. Okajima of SPring-8 for their help with the XAFS experiments. Mr. A. Hirai, Mr. N. Sato, Mr. H. Suzuki and Mr. S. Matsueda of Cataler Corp., and Mr. S. Mitachi and Mr. S. Araki of Hokko Chemical Industry Co. Ltd. are gratefully acknowledged for their cooperation in the industrialization of the catalyst. Gratitude is extended to Mr. K. Mitsumori, Mr. I. Takahashi, Mr. N. Kajita Mr. K. Yasuda, Mr. K. Naito, Mr. T. Ogawa and Mr. R. Iwasaki of Daihatsu Motor Co. Ltd. The XAFS Study in SPring-8 was supported by The Ministry of Education, Culture, Sports, Science and Technology; KAKENHI (15350090).

References

- [1] Y. Nishihata, J. Mizuki, T. Akao, H. Tanaka, M. Uenishi, M. Kimura, T. Okamoto, N. Hamada, *Nature* 418 (2002) 164.
- [2] H. Tanaka, I. Takahashi, M. Kimura, H. Sobukawa, in: Y. Izumi, H. Arai, M. Iwamoto (Eds.), *Science and Technology in Catalysts 1994*, Kodansya, Elsevier, Tokyo, 1995, p. 457.
- [3] H. Tanaka, M. Uenishi, I. Tan, M. Kimura, Y. Nishihata, J. Mizuki, SAE Paper.2001-1-1301, Society of Automotive Engineers, Warrendale, Pennsylvania, 2001.
- [4] H. Tanaka, M. Uenishi, I. Tan, M. Kimura, K. Dohmae, *Topics Catal.* 16/17 (1–4) (2001) 63.
- [5] H. Tanaka, in: M. Iwamoto (Ed.), *Kankyo Shokubai Handbook*, NTS, Tokyo, 2001, p. 320.
- [6] <http://snet.sntt.or.jp/imf/>: “The intelligent materials forum 1990”, The society of non-traditional technology.
- [7] *Platinum Interim Review*, Johnson Matthey, 2004.
- [8] N. Sato, H. Tanaka, I. Tan, M. Uenishi, N. Kajita, M. Taniguchi, K. Narita, M. Kimura, SAE Paper, 2003-01-0813, 2003.
- [9] H. Tanaka, M. Taniguchi, N. Kajita, M. Uenishi, I. Tan, N. Sato, K. Narita, M. Kimura, *Topics Catal.* 30/31 (2004) 389.
- [10] I. Tan, H. Tanaka, M. Uenishi, N. Kajita, M. Taniguchi, Y. Nishihata, J. Mizuki, SAE Paper, 2003-01-0812, 2003.
- [11] I. Tan, H. Tanaka, M. Uenishi, K. Kaneko, S. Mitachi, *J. Ceram. Soc. Jpn.* 113 (1) (2005) 71.
- [12] H. Tanaka, I. Tan, M. Uenishi, M. Taniguchi, M. Kimura, Y. Nishihata, J. Mizuki, *J. Alloys Compd.* 408–412 (2) (2006) 1071.
- [13] M. Taniguchi, M. Uenishi, I. Tan, H. Tanaka, M. Kimura, Y. Nishihata, J. Mizuki, SAE Paper, 2004-01-1272, 2004.
- [14] M. Uenishi, M. Taniguchi, H. Tanaka, M. Kimura, Y. Nishihata, J. Mizuki, T. Kobayashi, *Appl. Catal. B: Environ.* 57 (2005) 267.
- [15] H. Tanaka, M. Uenishi, M. Taniguchi, M. Kimura, Y. Nishihata, J. Mizuki, *Proceedings of the 13th ICC, Paris, July 11–16, 2004*, Poster No. 6-119.
- [16] H. Tanaka, I. Tan, M. Uenishi, M. Taniguchi, M. Kimura, Y. Nishihata, J. Mizuki, *Key Eng. Mater.* 317–18 (2006) 827.
- [17] H. Tanaka, *Catal. Surv. Asia* 9 (2) (2005) 63.
- [18] Y. Nishihata, J. Mizuki, H. Tanaka, M. Uenishi, M. Kimura, *J. Phys. Chem. Solid* 66 (2–4) (2005) 274.
- [19] M.A. Newton, B. Jyoti, A.J. Dent, S. Diaz-Moreno, S.G. Fiddy, J. Evans, *Chem. Phys. Chem.* 5 (2004) 1056.
- [20] K. Okumura, T. Kusakabe, S. Yokota, K. Kato, H. Tanida, T. Uruga, M. Niwa, *Chem. Lett.* 32 (2003) 7.
- [21] H. Tanaka, M. Yamamoto, SAE Paper, 960794, 1996.
- [22] H. Tanaka, M. Taniguchi, M. Uenishi, N. Kajita, I. Tan, Y. Nishihata and J. Mizuki, K. Narita, M. Kimura, K. Kaneko, *Angew. Chem. Inter. Edit.*, submitted for publication.
- [23] M.D. Smith, A.F. Stepan, C. Ramarao, P.E. Brennan, S.V. Ley, *Chem. Commun.* (2003) 2652.
- [24] S.P. Andrews, A.F. Stepan, H. Tanaka, S.V. Ley, M.D. Smith, *Adv. Synth. Catal.* 347 (2005) 647.